Journal of Materials Chemistry B

Accepted Manuscript

ROYAL SOCIETY OF CHEMISTRY

www.rsc.org/materialsB

Journal Name

RSCPublishing

COMMUNICATION

Enzyme-triggered supramolecular self-assemblies of platinum prodrug with enhanced tumor-selective accumulation and reduced systemic toxicity

Cite this: DOI: 10.1039/x0xx00000x

Received 00th January 2012,
Accepted 00th January 2012

DOI: 10.1039/x0xx00000x

www.rsc.org/

Huan Liu,[‡a] Yanli Li,[‡b] Zhonglin Lyu,[‡a] Yingbo Wan,[a] Xiaohong Li,[a] Huabing Chen,[b] Hong Chen[a] and Xinming Li[*a]

We reported the generation of a novel self-assembled prodrug of platinum (Pt) from short peptide derivative, a substrate of phosphatase for dephosphorylation reaction, and a Pt(IV) complex, which could undergo supramolecular self-assemblies with the presence of alkaline phosphatase, and perform controlled release of Pt(II) drug under reductive condition of tumor cell. This self-assembled prodrug showed significant antitumor growth effects on a breast cancer xenograft model based on 4T1 cells *in vivo*, but much lower toxicity towards kidney, liver, spleen and other major organs in mice than the free drug of cisplatin. Such improved antitumor efficacy could be ascribed to the localized and sustained release of Pt(II) anticancer drug from the supramolecular self-assemblies of the Pt(IV) prodrug which was triggered by phosphatases in tumor site.

Introduction

Cisplatin as a mainstay of platinum (Pt) drugs is widely employed in clinic for the treatment of various cancers including breast, ovarian, bladder, testicular, head and neck, and small cell lung cancers.[1] However, its clinical application is hindered by dose limiting toxicities and poor whole-body or cellular pharmacokinetic profiles during drug administration.[2] With the purpose of improving the therapeutic efficacy of cisplatin while decreasing its adverse side effects, various approaches have been taken in recent years, including the encapsulation of cisplatin inside different nanomaterials such as, nanoparticles, nanotubes, liposomes and polymers to prolong its half-life, reduce its side effects or improve drug delivery.[3] However, the extensive usages of these nanomaterials (e.g., metal nanoparticles, carbon nanotube and graphene-based nanomaterials) as drug carrier also raised certain biosafety concerns about their potential toxicities or unwanted side effects from long term of consideration.[4] Another promising strategy to minimize the side effects of cisplatin is to employ other analogues of Pt complexes, such as oxaliplatin, nedaplatin and lobaplatin, which ensure high kinetic inertness of Pt drug, but displayed less anticancer efficacy than cisplatin.[5]

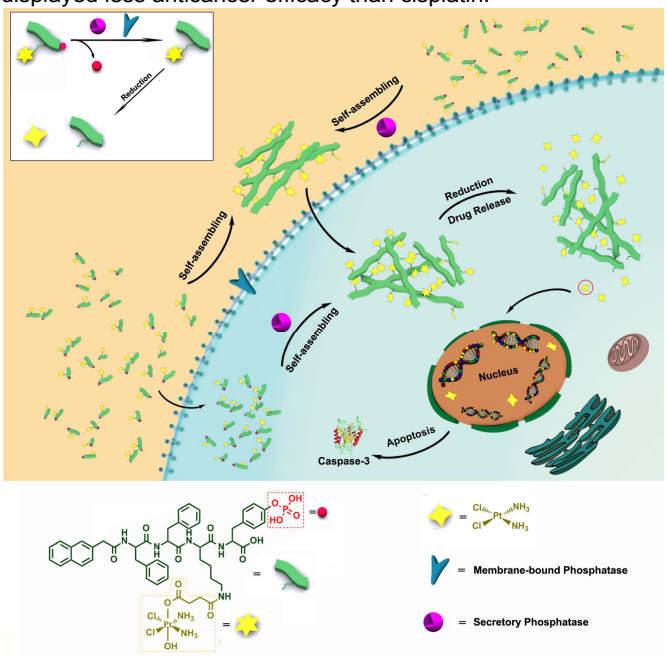

Scheme 1 The illustration of enzyme-triggered supramolecular self-assemblies of prodrug **1** for site-specific drug accumulation and controlled drug release in response to both phosphatases and redox conditions of tumor cells.

Most recently, self-assembled prodrug has emerged as a novel method for preparation of stimuli responsive biomaterials for drug delivery, and exhibited improved therapeutic efficacy in comparison with their parent drugs.[6] In this approach, covalent linkage of a parent drug to a small molecule motif of self-assembly generates a prodrug that undergoes tailored supramolecular self-assembly and performs controlled drug release in response to different biological cues.[7] Compared to

conventional drug delivery, self-assembled prodrug exhibited numerous advantages such as, high drug loading, enhanced sustained delivery, elimination of excipient-associated adverse effect and mitigation of the burst release of drug, which present a significant advancement in drug design and delivery.[8]

Like most of other small-molecular anticancer drugs, poor bioavailability of Pt drug is one the major problems that hinder its clinical applications. Upon administration, a large proportion of the drug is distributed throughout the whole body and only a small amount of it can reach the target for antitumor therapy.[9] Therefore, ensuring tumor-specific drug delivery or localized distribution of drug within tumor is very attractive strategy for improving the bioavailability of Pt drug, enhancing therapeutic efficacy and reducing toxicity,[10] and such selectivity can be achieved by exploiting the presence of enzymes or proteins up-regulated in tumor cells. Phosphatase, as a group of enzyme with enhanced activities in many cancer cells[11] and responsible for hydrolysis of phosphate ester groups from various protein and nonprotein substrates, have been widely exploited for cancer diagnostics and therapy.[12] Additionally, phosphatases also demonstrated the great potential to catalyze the formation of supramolecular self-assemblies from varied peptidic hydrogelaors.[13] In this study, we decide to take the advantage of the enzymatic activities of phosphatases *in vivo* to design a new amphiphilic Pt prodrug which can achieve drug accumulation and retention in tumor area through the in-situ formation of supramolecular self-assemblies triggered by locally expressed phosphatases.[11d] The occurrence of supramolecular self-assemblies of Pt prodrug can not only enhance tumor-specific drug accumulation and retention, and avoid undesirable bindings and side reactions of Pt prodrug with a vast of number of biomolecules, but also ensure prolonged and sustained Pt(II) drug release under reductive condition of tumor cells for antitumor therapy.

Herein, we integrated short peptide derivative, a substrate of phosphatase for dephosphorylation reaction, and a Pt(IV) complex (*c*,*c*,*t*-[$Pt(NH_3)_2Cl_2(OH)_2$]) to generate a novel self-assembled Pt(IV) prodrug, which can not only undergo supramolecular self-assemblies with the presence of phosphatase, but also display a self-sustained release profile of Pt(II) drug (*cis*-[$Pt(NH_3)_2(Cl)_2$]) under reductive condition similar to cytosolic environment of tumor cells, and induced the apoptosis of cancer cell in vitro (Scheme 1). Pt(IV), a newly developed derivative of cisplatin, exhibited great potentials work as the prodrug of Pt(II) because of high kinetic inertness, low off-target reactivity, easy functionalization via two axial ligands and latent cytotoxicity susceptible to intracellular reduction conditions.[14] More importantly, in vivo tumor inhibition examination, biodistribution and hematoxylin and eosin (H&E) staining demonstrated that this self-assembled prodrug exhibited comparable antitumor growth effects owing to the enhanced drug accumulation in tumor site, and much lower systemic toxicity, when compared with the free drug of cisplatin. Such improved antitumor efficacy could be ascribed to the localized and sustained release of Pt(II) anticancer drug from the supramolecular self-assemblies of Pt(IV) prodrug triggered by phosphatases in tumor site. We expected that the concept illustrated in our work could lead to new studies to improve the therapeutic efficacy of Pt drugs by reducing toxic side effects, but without compromising their antitumor activity.

Results & discussion

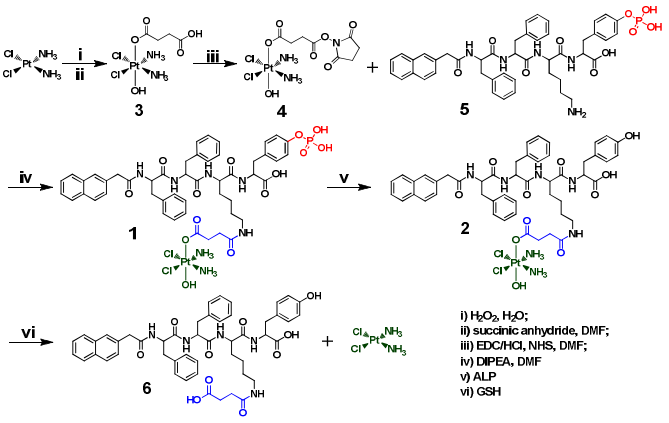

Scheme 2 The molecular structure and synthetic routes towards prodrug **1**, the supramolecular hydrogelator precursor, and the enzymatic conversion for the generation of prodrug **2**, the supramolecular hydrogelator, by phosphatase.

Scheme 2 shows the molecular structure and synthesis route toward prodrug **1**, which was prepared from short peptide derivative **5** and Pt(IV) complex (**3**). **5** was synthesized by following typical solid-phase synthesis procedures (Fig. S1), which consisted of a naphthyl group, two phenylalanines, one lysine and one tyrosine phosphate residue in its molecular structure. The tyrosine phosphate group worked as an effective substrate of phosphatase for dephosphorylation reaction to induce the supramolecular self-assembly of **5**.[15] The Pt(IV) complex (**3**) was prepared from commercially available anticancer drug cisplatin through hydrogen peroxide oxidation and subsequent succinic anhydride treatment. After being activated by N-hydroxysuccinimide (NHS), **3** was converted to **4**, which then reacted with the epsilon amino group of lysine residue on **5** to afford prodrug **1** (Fig. S4).

To evaluate the sensitivity of the obtained prodrug **1** towards phosphatase for the formation of supramolecular self-assemblies, we dissolved 2 mg of **1** in 200 μL PBS buffer at pH 7.4 to make a clear solution with final concentration at 1.0 wt%. After treated with 1 unit of alkaline phosphatase, the clear solution of **1** turned to translucent hydrogel in 2 h at room temperature via the transformation of prodrug **1** to prodrug **2** through dephosphorylation reaction catalyzed by alkaline phosphatase. And the afforded hydrophobic entity (**2**) can easily undergo supramolecular self-assemblies through aromatic-aromatic and hydrogen bonding interactions for the formation of hydrogel. To examine the extent of the self-assembly of prodrug **2** from enzymatic conversion, we used transmission electron

microscopy (TEM) and atomic force microscopy (AFM) to study the structural morphologies of the hydrogel. As shown in Fig. 1A and 1B, we observed the formation of well-defined nanofibrous structures from prodrug **2**, with a width of approximately 10 nm. With the application of oscillatory rheology, we tested the viscoelastic properties of the hydrogels formed from produrg **2**.

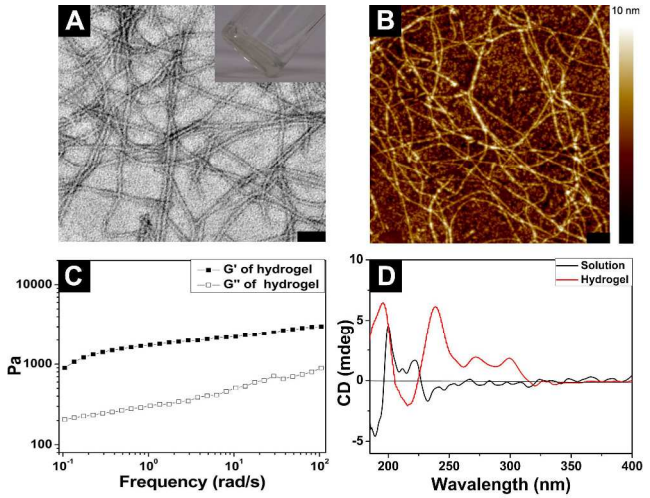

Fig. 1 The (A) TEM image, (B) AFM image and rheological study of the supramolecular hydrogel (the inset image in Fig. 1A) formed by prodrug **1** (1.0 wt%) triggered by alkaline phosphatase; (D) CD spectra of the precursor solution of prodrug **1** before and after the addition of alkaline phosphatase. (Scale bar = 50 nm).

As displayed in Fig. 1C, the hydrogel exhibited typical solid-like rheological behavior with the storage modulus (G') greater than the loss modulus (G'') within the investigated oscillating strain limit. The secondary structures formed by the prodrug **2** were probed by circular dichroism (CD) spectroscopy during its supramolecular self-assembly. According to the CD spectra shown in Fig. 1D, we observed a positive peak near 195 nm and a negative peak around 220 nm from the hydrogel of prodrug **2**, indicating the adoption of β-sheet-like structure during the self-assembly of prodrug **2**, while the solution of prodrug **1** before the addition of phosphatase displayed a negative peak near 190 nm and a positive peak around 200 nm, which was consistent with the absence of regularly secondary structures without the presence of phosphatases. These results indicated that our designed prodrug **1** exhibited high sensitivity toward phosphatase to undergo supramolecular self-assemblies through the generation of prodrug **2**, which then tended to arrange itself into β-sheet-like structure during the formation of supramolecular nanofibers/hydrogel.

In order to test the potential of the supramolecular nanofibers/hydrogels of **2** to work as effective reservoir for controlled release of Pt(II) drug under reductive condition, we put the hydrogel of prodrug **2** into PBS buffer (pH=7.4) containing different concentrations of GSH (0, 5 μM, 250 μM and 5 mM), and analyzed the controlled release profile of Pt(II) drug stimulated by GSH, in which the Pt(IV) entity linked to hydrogelator underwent transformation to Pt(II) through the elimination of its axial dihydroxy ligands.[16] During the course of our study, we adopted an easy and sensitive method to quantify the amount of Pt(II) released from the hydrogel. In the approach, the released Pt(II) residues can be reduced to Pt(0) properly with the presence of PPh_3, and then form Pt(0)-PPh_3 complex to turn on the fluorescence of dichlorofluorescein through deprotection reaction of the allylic group (Fig. 2A and S7).[17] By fitting the data of fluorescence intensities of solution and the known concentrations of Pt(II), we got a linear relationship between Pt(II) concentrations and fluorescence intensities, which was used for easy determination of the amount of Pt(II) released from the hydrogel.

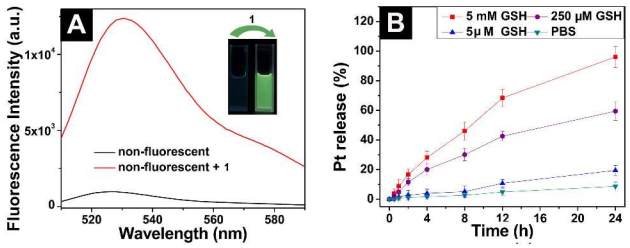

Fig. 2 (A) Fluorescence emission spectra of dichlorofluorescein solution with and without the presence Pt(II) (Ex: 493 nm, Em: 530 nm). Inset: Corresponding photographs taken under 365 nm UV light; (B) The controlled release profile of Pt(II) drug from the hydrogel of prodrug **2** stimulated by the presence of different concentrations of glutathione (GSH) in PBS buffer (10 mM, pH 7.4).

Based on the standard curve shown in Fig. S7B, we checked the amounts of Pt(II) released from hydrogel with time. From the graph shown in Fig. 2B, we found that the rate of Pt(II) drug released from the hydrogel increased with the concentration of GSH in PBS buffer. When a 5 μM GSH solution was used, which is concentration of GSH in extracellular plasma,[18] the release rate was very slow and only 20% of the drug was released in 24 hrs. However, the concentration of GSH was increased to 5 mM, close to the concentration of GSH (3~10 mM) inside of cancer cells,[18] a steady Pt(II) drug-release behavior was observed during the time course analysis (0, 0.5, 1, 2, 4, 8, 12 and 24 hrs), and almost 100% of immobilized Pt(IV) drug was released properly in 24 hrs, which was also confirmed by inductively coupled plasma mass spectrometry analysis (ICP-MS). These data indicated that the supramolecular nanofibers/hydrogel formed from prodrug **2** can perform controlled release of Pt(II) drug in different profiles according to the reductive conditions of extracellular and cytosolic environments.[19]

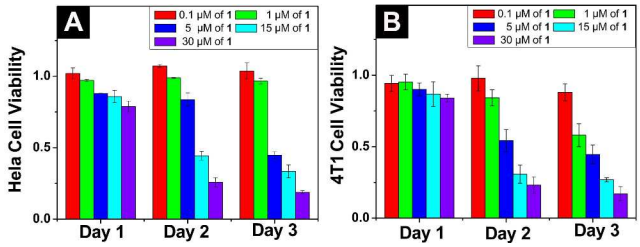

Fig. 3 Three-day cytotoxicities of prodrug **1** towards (A) Hela cell and (B) 4T1 cell at different concentrations (e.g., 0.1, 1.0, 5.0, 15 and 30 μM, respectively).

The cytotoxic profiles of **1** towards both Hela cells (human cervical carcinoma cell line) and 4T1 cells (mouse breast cancer cell line) were investigated by standard MTT assays. According to the data shown in Fig. 3, we found that compound **1** was toxic towards both HeLa and 4T1 cells, and its cytotoxicities were highly dependent on the concentrations of compound and the incubation time (e.g., 24, 48 and 72 h). For example, the cytotoxicity of **1** was low in the first 24 h, with the half-maximal inhibitory concentration (IC_{50}) more than 30 μM towards both Hela cells and 4T1 cell, confirming the kinetic inertness of our prodrug. However, with extending the incubation time to 48 and 72 h, we observed a dramatic decrease of viability of cells, and the IC_{50} values were decreased to 13.6 and 4.6 μM for Hela cells, and 6.9 μM and 3.4 μM for 4T1 cells, respectively. In the control experiment (Fig. S8), the free drug of cisplatin displayed extremely high cytotoxicity towards both Hela and 4TI cells with IC_{50} values at 7.3 and 8.6 μM, respectively, while compound **5** did not show obvious cytotoxicity towards Hela cells, even in much higher concentration at 100 μM and 72 h exposure, indicating the biocompatibility of the short peptide derivative **5**, which was suitable to work as the scaffold to prepare the self-assembled prodrug.

Apoptosis is one of the most widely investigated processes of cancer cell death by anti-cancer drugs in cancer therapy.[20] With the purpose of investigating that the programmed cell death by

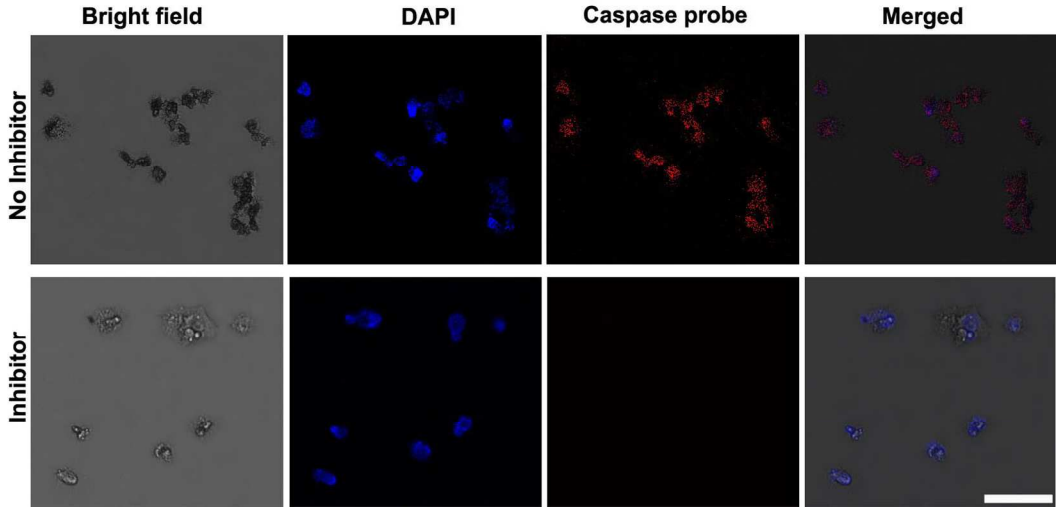

Fig. 4 Live-cell fluorescent apoptosis imaging in Hela cells pretreated by prodrug **1** with or without the presence of caspase-3 inhibitors. Blue: nuclear staining dye (DAPI); red: caspase-3 probe (sulforhodamine-DEVD-FMK). (Scale bar = 75 μm).

prodrug **1** was resulted from drug-induced apoptosis, a cytotoxic mechanism study was conducted through real-time apoptosis imaging. Since the major biochemical features of apoptosis are the activation of intracellular caspases, and caspase-3 has been identified as a key effector of cell apoptosis and an important indicator of the cell's entry point into the apoptotic pathway,[21] confocal fluorescence microscopy and fluorescent caspase-3 activation probe (sulforhodamine-DEVD-FMK) were used to examine the occurrence of apoptosis. As shown in Fig. 4, Hela cells pretreated with prodrug **1** showed strong fluorescence signals after incubating with the probe, indicative of the presence of caspase-3 activity in the apoptotic cells. On the other hand, an extremely low fluorescence signal was observed in the control experiment, where the prodrug **1** pretreated cells were incubated with both the fluorescent probe and caspase-3 inhibitor. The cellular imaging clearly suggested the apoptotic pathway for the programmed cell death induced by prodrug **1**.

To examine the antitumor activity of **1** *in vivo*, we conducted comparative efficacy studies in 4T1 tumor-bearing mice. The mice were randomly divided into 3 groups and treated with PBS buffer, cisplatin and **1**, respectively, by direct intratumoral injection every 48 hours (e.g., 0, 2, 4 and 6 days). The relative tumor volume changes as a function of time were plotted and shown in Fig. 5A. Mice treated with **1** and cisplatin, experienced rapid and significant tumor reduction in the first eight days when the drugs were administrated, and the tumor began to grow again with time in the rest days of post injection, but at a much slower rate than that in PBS control group. The final volumes of tumors in the cisplatin and **1** group were 11.21±3.5 mm^3 and 23.80±9.8 mm^3, respectively, which was much smaller than those in the PBS group (752.41±19 mm^3), indicating that **1** can induced similar antitumor effects on 4T1 cancer cells as cisplatin did *in vivo*. In addition, from the data of body weight changes of mice shown in Fig. 5C, we found that the body weight of mice in the **1** group can keep stabilized when the drug was administrated, and increased gradually during the time of post injection, while the mice treated with cisplatin experienced an obvious drop of body weight during drug administration, which indicated the similar antitumor effects and much lower toxicity of **1** towards mice than that of cisplatin.

In addition, we next investigated the biodistribution of Pt drug between tumor and major organs (e.g., kidney, lung, spleen, liver and heart) of the mice by using ICP-MS. From the biodistribution profiles of cisplatin and **1** shown in Fig. 5D, we found that,

compared with the mice injected with free cisplatin, the mice treated with **1** show increased proportion of Pt drug accumulated in tumor site (16.3341±0.57893 ng/mg tissue), and relatively lower amount of Pt drug was observed in kidney, liver and other major organs, indicating the site-specific accumulation of prodrug **1** at tumor site for antitumor therapy. And this data are also consistent with our earlier observations of the low toxicity of **1** to mice because of the local distribution of prodrug **1** in tumor tissue. With the purpose of evaluating the antitumor efficacy of prodrug **1**, the tumors and major organs (e.g., kidney, lung, spleen, liver and heart) were dissected from mice of different groups and stained by H&E for pathological analysis. From the histological analysis data of tumor tissues shown in Fig. 5E, we found that the tumors of the PBS group were composed of tightly packed tumor cells, indicating the rapid tumor growth. In contrast, the tumor cellularity of the cisplatin or prodrug **1** group exhibited typical apoptotic characteristics, such as extensive fragmentation and nuclear shrinkage. And a large area of tumor necrosis was observed in the tumor tissue of cisplatin group, while the prodrug **1** group displayed a relative lower necrotic level.

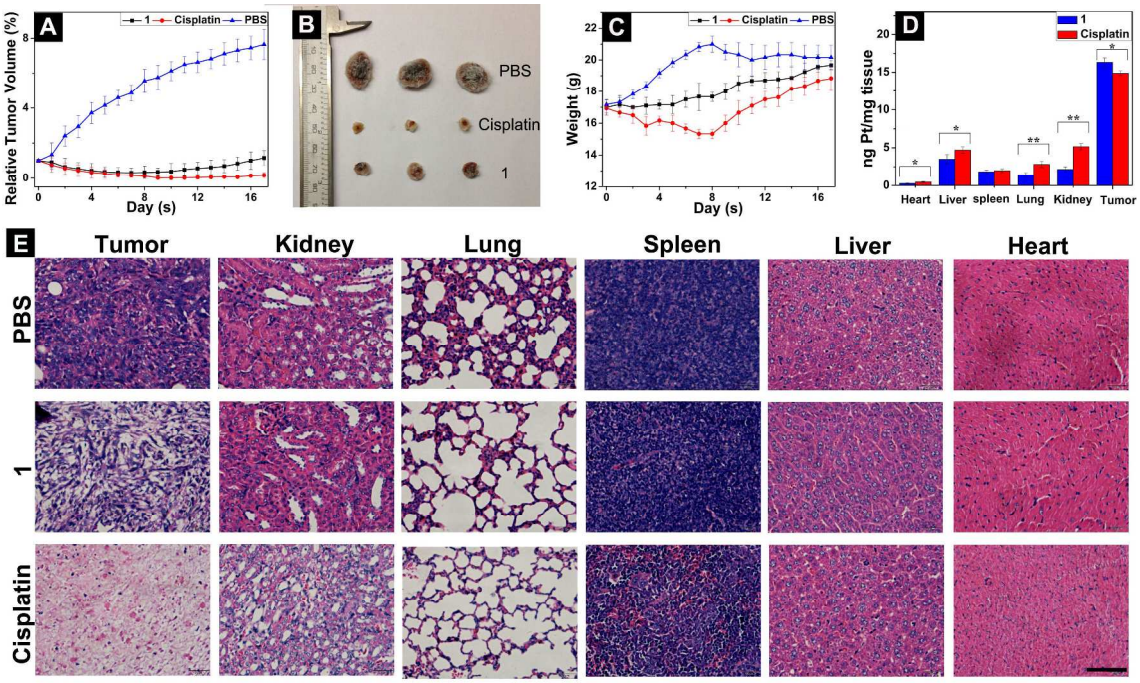

Fig. 5 (A and B) *In vivo* tumor volume changes of 4T1 breast cancer xenografts in different groups after various treatments by PBS buffer, cisplatin and **1**, respectively; (C) body weight changes with time of 4T1 tumor-bearing mice under different treatments by PBS buffer, cisplatin and **1**, respectively; (D) Bio-distribution profiles of cisplatin and **1** in tumor, kidney, lung, spleen, liver and heart of 4T1 tumor-bearing mice (*: P<0.05, **: P<0.01); (E) representative H&E staining images of tumor and major organs including kidney, lung, spleen, liver and heart collected from 4T1 tumor-bearing mice treated by PBS buffer, cisplatin and **1**, respectively. Error bars represent standard deviations. Scale bar=100 μm.

Since low adverse-effect is a major issue of consideration for *in vivo* application of chemotherapy, histopathological examinations of major organs (e.g., kidney, lung, spleen, liver and heart) were also performed (Fig. 5E). Histological analysis of the tissues from different organs showed that no significant changes were detected in the organs from the PBS group. However, the mice treated with cisplatin displayed noticeable pathological changes of organ tissues in kidney, spleen and liver. In contrast, treatment of the tumor-bearing mice with prodrug **1** did not result in obvious damages to the major organs that we examined, suggesting the low toxicity of prodrug **1** which is suitable for long-term administration.

Conclusions

In summary, we integrated a Pt(IV) complex and a short peptide to prepare a novel self-assembled prodrug with enzyme and redox dual stimuli responsiveness for supramolecular self-assembly and controlled drug release. In vitro studies demonstrated that this prodrug can self-assembled to form supramolecular nanofibers/hydrogels through dephosphorylation reaction catalyzed by alkaline phosphatase, and displayed a self-sustained release profile of Pt(II) drug under reductive condition similar to cytosolic environment of tumor cells. In vivo biodistribution, tumor inhibition examination and hematoxylin and eosin (H&E) staining demonstrated that the self-assembled anticancer prodrug exhibited improved efficacy in enhancing drug accumulation in tumor, restricting tumor growth and reducing systemic toxicity compared to free drug of cisplatin. Due to many advantages of our approach, we expected that the concept illustrated in our work could lead to new studies to improve the therapeutic efficacy of Pt drugs by reducing toxic side effects, but without compromising their antitumor activity.

Acknowledgements

We thank the National Science Fund for Distinguished Young Scholars (201125418) to H. Chen, the National Natural Science Foundation of China (21334004, 21344002 and 21305098) to H. Chen, XM. Li and XH. Li, respectively, the Priority Academic Program Development of Jiangsu Higher Education Institutions (PAPD) and the Key Lab of Health Chemistry and Molecular Diagnosis of Suzhou to support this work.

Notes and references

[a] *College of Chemistry, Chemical Engineering and Materials Science, Soochow University, Suzhou, China 215123. Tel: 86-0512-6588-2917. E-mail: xinmingli@suda.edu.cn.*

[b] *College of Pharmaceutical Sciences, Soochow University, Suzhou, China 215123.*

‡ These authors contribute equally to this work.

† Electronic Supplementary Information (ESI) available: Detailed reaction conditions and procedures for the synthesis of compound **1**, **2**, **3**, **4** and **5** and their corresponding NMR and MS spectra. See DOI: 10.1039/c000000x/

1. a) E. R. Jamieson and S. J. Lippard, *Chem. Rev.*, 1999, **99**, 2467-2498; b) L. Kelland, *Nat. Rev. Cancer*, 2007, **7**, 573-584.
2. D. Wang and S. J. Lippard, *Nat. Rev. Drug Discovery*, 2005, **4**, 307-320.
3. a) R. Haag and F. Kratz, *Angew. Chem. Int. Ed.*, 2006, **45**, 1198-1215; b) R. P. Feazell, N. Nakayama-Ratchford, H. Dai and S. J. Lippard, *J. Am. Chem. Soc.*, 2007, **129**, 8438-+; c) W. J. Rieter, K. M. Pott, K. M. L. Taylor and W. Lin, *J. Am. Chem. Soc.*, 2008, **130**, 11584-11585; d) N. Kolishetti, S. Dhar, P. M. Valencia, L. Q. Lin, R. Karnik, S. J. Lippard, R. Langer and O. C. Farokhzad, *Proc. Nat. Acad. Sci. U.S.A.*, 2010, **107**, 17939-17944; e) C. R. Patra, R. Bhattacharya and P. Mukherjee, *J. Mater. Chem.*, 2010, **20**, 547-554; f) P. Sengupta, S. Basu, S. Soni, A. Pandey, B. Roy, M. S. Oh, K. T. Chin, A. S. Paraskar, S. Sarangi, Y. Connor, V. S. Sabbisetti, J. Kopparam, A. Kulkarni, K. Muto, C. Amarasiriwardena, I. Jayawardene, N. Lupoli, D. M. Dinulescu, J. V. Bonventre, R. A. Mashelkar and S. Sengupta, *Proc. Nat. Acad. Sci. U.S.A.*, 2012, **109**, 11294-11299; g) Y. Kuang, J. Liu, Z. Liu and R. Zhuo, *Biomaterials*, 2012, **33**, 1596-1606; h) S. Aryal, C.-M. J. Hu and L. Zhang, *Chem. Commun.*, 2012, **48**, 2630-2632; i) H. S. Oberoi, N. V. Nukolova, A. V. Kabanov and T. K. Bronich, *Adv. Drug Deliv. Rev.*, 2013, **65**, 1667-1685; j) X. Wang and Z. Guo, *Chem. Soc. Rev.*, 2013, **42**, 202-224; k) Y. Min, J. Li, F. Liu, E. K. L. Yeow and B. Xing, *Angew. Chem. Int. Ed.*, 2014, **53**, 1012-1016; l) Y. Wang, J. Zhou, L. Qiu, X. Wang, L. Chen, T. Liu and W. Di, *Biomaterials*, 2014, **35**, 4297-4309; m) J.-X. Chen, X.-D. Xu, W.-H. Chen and X.-Z. Zhang, *ACS Appl. Mater. Interfaces*, 2014, **6**, 593-598; n) C. F. Chin, S. Q. Yap, J. Li, G. Pastorin and W. H. Ang, *Chem. Sci.*, 2014, **5**, 2265-2270.
4. a) A. Nel, T. Xia, L. Madler and N. Li, *Science*, 2006, **311**, 622-627; b) S. Sharifi, S. Behzadi, S. Laurent, M. L. Forrest, P. Stroeve and M. Mahmoudi, *Chem. Soc. Rev.*, 2012, **41**, 2323-2343.
5. a) R. J. Knox, F. Friedlos, D. A. Lydall and J. J. Roberts, *Cancer Res.*, 1986, **46**, 1972-1979; b) R. S. Go and A. A. Adjei, *J. Clin. Oncol.*, 1999, **17**, 409-422.
6. a) J. B. Matson and S. I. Stupp, *Chem. Commun.*, 2012, **48**, 26-33; b) H. Wang, L. Lv, G. Xu, C. Yang, J. Sun and Z. Yang, *J. Mater. Chem.*, 2012, **22**, 16933-16938; c) A. G. Cheetham, P. Zhang, Y.-a. Lin, L. L. Lock and H. Cui, *J. Am. Chem. Soc.*, 2013, **135**, 2907-2910; d) J. Li, Y. Gao, Y. Kuang, J. Shi, X. Du, J. Zhou, H. Wang, Z. Yang and B. Xu, *J. Am. Chem. Soc.*, 2013, **135**, 9907-9914; e) G. Verma and P. A. Hassan, *Phys. Chem. Chem. Phys.*, 2013, **15**, 17016-17028; f) M. R. Reithofer, K.-H. Chan, A. Lakshmanan, D. H. Lam, A. Mishra, B. Gopalan, M. Joshi, S. Wang and C. A. E. Hauser, *Chem. Sci.*, 2014, **5**, 625-630; g) M. Yang, D. Xu, L. Jiang, L. Zhang, D. Dustin, R. Lund, L. Liu and H. Dong, *Chem. Commun.*, 2014, **50**, 4827-4830.
7. a) R. J. Mart, R. D. Osborne, M. M. Stevens and R. V. Ulijn, *Soft Matter*, 2006, **2**, 822-835; b) P. K. Vemula, G. A. Cruikshank, J. M. Karp and G. John, *Biomaterials*, 2009, **30**, 383-393; c) Y. Chen and G. Liang, *Theranostics*, 2012, **2**, 139-147.
8. P. K. Vemula, N. Wiradharma, J. A. Ankrum, O. R. Miranda, G. John and J. M. Karp, *Curr. Opin. Biotechnol.*, 2013, **24**, 1174-1182.
9. A. R. Timerbaev, C. G. Hartinger, S. S. Aleksenko and B. K. Keppler, *Chem. Rev.*, 2006, **106**, 2224-2248.
10. J. S. Butler and P. J. Sadler, *Curr. Opin. Chem. Biol.*, 2013, **17**, 175-188.
11. a) N. A. Elson and R. P. Cox, *Biochem. Genet.*, 1969, **3**, 549-&; b) K. G. Nelson, J. S. Haskill, S. Sloan, J. M. Siegfried, G. P. Siegal, L. Walton and D. G. Kaufman, *Cancer Res.*, 1987, **47**, 2814-2820; c) C.-C. Wu, C.-W. Hsu, C.-D. Chen, C.-J. Yu, K.-P. Chang, D.-I. Tai, H.-P. Liu, W.-H. Su, Y.-S. Chang and J.-S. Yu, *Mol. Cell. Proteomics*, 2010, **9**, 1100-1117; d) C. E. Nunes-Xavier, J. Martin-Perez, A. Elson and R. Pulido, *Biochim. Biophys. Acta, Rev. Cancer*, 2013, **1836**, 211-226.
12. a) M. M. Tiscornia, M. A. Riera, M. A. Lorenzati and P. D. Zapata, *Recent patents on DNA & gene sequences*, 2010, **4**, 46-51; b) Y. Kuang, J. Shi, J. Li, D. Yuan, K. A. Alberti, Q. Xu and B. Xu, *Angew. Chem. Int. Ed.*, 2014, **53**, 1-6.
13. a) Z. Yang, G. Liang and B. Xu, *Acc. Chem. Res.*, 2008, **41**, 315-326; b) Y. Gao, C. Berciu, Y. Kuang, J. Shi, D. Nicastro and B. Xu, *ACS nano*, 2013, **7**, 9055-9063; c) M. C.-L. Yeung and V. W.-W. Yam, *Chem. Sci.*, 2013, **4**, 2928-2935.
14. a) H. Song, H. Xiao, Y. Zhang, H. Cai, R. Wang, Y. Zheng, Y. Huang, Y. Li, Z. Xie, T. Liu and X. Jing, *J. Mater. Chem.*, 2013, **1**, 762-772; b) H. Xiao, R. Qi, S. Liu, X. Hu, T. Duan, Y. Zheng, Y. Huang and X. Jing, *Biomaterials*, 2011, **32**, 7732-7739; c) H. Xiao, L. Yan, Y. Zhang, R. Qi, W. Li, R. Wang, S. Liu, Y. Huang, Y. Li and X. Jing, *Chem. Commun.*, 2012, **48**, 10730-10732.
15. Y. Gao, Y. Kuang, Z.-F. Guo, Z. Guo, I. J. Krauss and B. Xu, *J. Am. Chem. Soc.*, 2009, **131**, 13576-+.
16. M. D. Hall and T. W. Hambley, *Coord. Chem. Rev.* , 2002, **232**, 49-67.
17. B. Ahn, J. Park, K. Singha, H. Park and W. J. Kim, *J. Mater. Chem. B*, 2013, **1**, 2829-2836.
18. A. Meister, *J. Biol. Chem.*, 1994, **269**, 9397-9400.

19. a) H. Xiao, H. Song, Q. Yang, H. Cai, R. Qi, L. Yan, S. Liu, Y. Zheng, Y. Huang, T. Liu and X. Jing, *Biomaterials*, 2012, **33**, 6507-6519; b) H. Xiao, H. Song, Y. Zhang, R. Qi, R. Wang, Z. Xie, Y. Huang, Y. Li, Y. Wu and X. Jing, *Biomaterials*, 2012, **33**, 8657-8669.
20. J. F. R. Kerr, C. M. Winterford and B. V. Harmon, *Cancer*, 1994, **73**, 2013-2026.
21. a) D. R. Green, *Cell*, 1998, **94**, 695-698; b) N. A. Thornberry and Y. Lazebnik, *Science*, 1998, **281**, 1312-1316.

Table of Content:

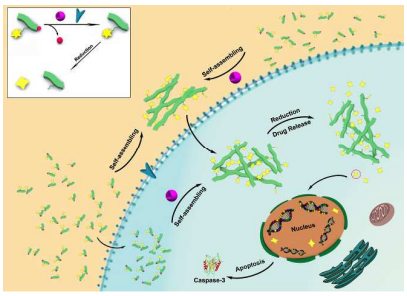

A self-assembled Pt prodrug with enhanced drug accumulation in tumor area was achieved through the catalysis of locally expressed enzyme.